JPET Fast Forward. Published on February 10, 2004 as DOI:10.1124/jpet.103.063289

Pharmacokinetics of Recombinant Human Leukemia Inhibitory Factor in Sheep

Alicia M. Segrave*, Donald E. Mager*, Susan A. Charman, Glenn A. Edwards and Christopher J.H. Porter.

Department of Pharmaceutics, Victorian College of Pharmacy, Monash University, Parkville, Victoria, Australia (A.M.S., S.A.C., C.J.H.P.)

National Institute on Aging, NIH, Gerontology Research Center, Baltimore, Maryland (D.E.M.)

Department of Veterinary Sciences, University of Melbourne, Werribee, Victoria, Australia (G.A.E.)

Running Title: Pharmacokinetics of rhLIF in Sheep

Corresponding Author: Susan A. Charman, Ph.D., Department of Pharmaceutics, Victorian College of Pharmacy, Monash University, 381 Royal Parade, Parkville, Victoria 3052, Australia. Phone: +61 3 99039626. Fax: +61 3 99039627. E-mail: susan.charman@vcp.monash.edu.au

Text pages: 34

Tables: 3

Figures: 3

References: 40

Abstract: 245 words

Introduction: 703 words

Discussion: 1497

Abbreviations: A_D, amount of drug in the absorption delay compartment; A_P, amount of drug in the central compartment; A_T, amount of drug in the tissue compartment; AUC, total area under the plasma drug concentration-time curve; CL, total systemic drug clearance; C_{max}, maximum plasma concentration; C_p^0, plasma concentration at time zero; D_{SC}, subcutaneous dose; D_{IV}, intravenous dose; ELISA, enzyme-linked immunosorbent assay; k_{a1}, first-order absorption rate constant from SC site to delay compartment ; k_{a2}, first-order transfer rate constant from delay compartment to central compartment; K_d, equilibrium dissociation constant; k_{deg}, first-order rate constant for degradation of R; k_e, first-order drug elimination from the central compartment; k_{int}, first-order rate of RC internalization and degradation; k_{nsb}, first-order rate constant for

JPET Fast Forward. Published on February 10, 2004 as DOI: 10.1124/jpet.103.063289
This article has not been copyedited and formatted. The final version may differ from this version.

non-specific binding process; k_{off}, first-order rate constant for dissociation of RC; k_{on}, second-order rate constant for formation of RC; k_{syn}, zero-order receptor production rate; LIF, leukemia inhibitory factor; R, amount of free (unoccupied) receptor; RC, amount of drug-receptor complex; rhLIF, recombinant human leukemia inhibitory factor; R_m, initial receptor density; $t_{1/2}$, terminal phase half-life; V_c, volume of the central compartment; V_{ss}, steady-state volume of distribution.

Section: Absorption, Distribution, Metabolism, & Excretion

ABSTRACT

The pharmacokinetics of recombinant human leukemia inhibitory factor (rhLIF) were investigated following IV and SC administration of a wide range of dose levels. Parallel studies were conducted where single IV bolus doses of 12.5, 25, 100, 250, 500 or 750 µg/kg rhLIF (n=2) or SC doses of 10, 20 or 50 µg/kg rhLIF (n=4) were administered to sheep. Blood samples were collected for up to 24 hours post-dosing and the plasma concentrations of rhLIF were analysed by ELISA. Non-compartmental analysis demonstrated an increase in the terminal elimination half-life (from 0.27 to 2.29 h) and a decrease in systemic clearance (from 5.18 to 1.09 mL/min/kg) with increasing IV doses of rhLIF, suggesting nonlinear pharmacokinetic behaviour. A greater than proportional increase in the area under the plasma concentration-time curve with dose also indicated significantly nonlinear pharmacokinetics after SC administration. A mechanistic compartmental model was developed to characterise the pharmacokinetics of rhLIF. The key feature of the model accounting for the nonlinear pharmacokinetic behaviour of rhLIF was high affinity, saturable receptor binding and subsequent cellular internalization and degradation. The apparent total density of LIF cell surface receptors and receptor turnover dynamics were included in the model, along with non-specific binding and linear elimination from the systemic circulation. The absorption of rhLIF from the SC injection site into the systemic circulation was characterized by a first-order absorption process via a delay compartment. The proposed model well captured the complex pharmacokinetic profiles of rhLIF following both IV and SC administration.

Leukemia inhibitory factor (LIF) is a 180 amino acid glycoprotein of the interleukin-6 type cytokine family. The name LIF was originally derived from the ability of the cytokine to induce macrophage maturation and suppress the clonogenicity of the murine monocytic leukemia cell line, M1 (Gearing et al., 1987). LIF acts on a wide range of cell types and displays remarkable functional diversity. LIF has been demonstrated to play a role, either directly or synergistically, in hematopoiesis, thrombopoiesis, reproduction, bone metabolism, inflammatory responses and neuropoiesis (Hilton and Gough, 1991a; Waring, 1997), and consequently, a number of potential therapeutic uses for LIF have been proposed. Initial clinical interest focused on its use in neurological conditions, in particular, chemotherapy-induced peripheral neuropathy (Kurek, 2000). Currently, LIF is under investigation for the treatment of infertility as it has been shown to enhance embryonic implantation (Stewart et al., 1992).

Native LIF produced by mammalian cells is highly basic (pI=9.15) and has a reported molecular weight in the range of 32-67 kDa. The heterogeneity in molecular weight has been attributed to extensive and variable glycosylation (Hilton, 1992). The recombinant form of human LIF (rhLIF) produced in *E. coli* is not glycosylated and has a molecular weight of 19.71 kDa. Glycosylation does not appear to be necessary for the biological actions of LIF (Williams et al., 1988) although it may alter the stability of the molecule both *in vitro* and *in vivo* (Hilton et al., 1991b; Yamamoto-Yamaguchi et al., 1992). LIF exerts its actions by binding to a specific cell surface receptor complex, comprised of the LIF receptor β chain (LIFRβ) and the gp130 receptor chain (Gearing et al., 1992). When LIF binds to the receptor complex, the two receptor components dimerise initiating signal transduction.

There are very few reports describing the pharmacokinetics of LIF. An initial study in mice showed that when administered intravenously at a single dose level, the plasma concentrations of murine LIF declined in a biexponential manner with a rapid initial distribution phase and a more prolonged terminal phase (Hilton et al., 1991b). Recent data obtained in patients with advanced cancer indicated that the absorption of rhLIF after SC administration was variable, with maximum plasma concentrations occurring 10 to 120 minutes post-dosing (Gunawardana et al., 2003). The terminal phase half-life of approximately 2 hours appeared to be independent of dose, however, there was a disproportionate increase in AUC and C_{max} with dose indicating nonlinearity in the pharmacokinetics of rhLIF. The authors suggested that the nonlinearity was probably due to increased bioavailability of rhLIF at higher SC doses, but also recognised that this finding may be a consequence of reduced clearance.

Several studies have attributed nonlinear disposition of cytokines to their high affinity, low-capacity binding to pharmacological targets on cell surfaces followed by internalization and subsequent degradation (Sugiyama and Hanano, 1989; Mager and Jusko, 2001). Protein clearance by receptor-mediated endocytosis has been demonstrated for a number of proteins that exhibit nonlinear plasma kinetics including erythropoietin (Chapel et al., 2001), granulocyte colony stimulating factor (Terashi et al., 1999) and hepatocyte growth factor (Liu et al., 1995). Additional mechanisms such as non-specific renal and hepatic elimination processes and proteolytic degradation may also contribute to the removal of cytokines from the systemic circulation (Ferraiolo et al., 1992).

The purpose of the present study was to evaluate the pharmacokinetics of rhLIF administered intravenously and subcutaneously over a wide range of dose levels. Sheep

were chosen as the study species because sheep and human LIF display a high degree of amino acid sequence homology (88%) and structural identity (Willson et al., 1992). This feature is important to obtain pharmacokinetic data reflective of that in humans as the binding of cytokines to pharmacological receptors may strongly influence disposition (Sugiyama and Hanano, 1989). Previous studies with recombinant human proteins including human growth hormone (Charman et al., 2000) and leptin (McLennan et al., 2003) have demonstrated the utility of the sheep model to produce pharmacokinetic parameters comparable to those in humans. Using the data generated in the present study, a mechanistic model was developed to describe the pharmacokinetics of rhLIF. The model aided interpretation of the likely mechanisms of absorption and clearance of rhLIF and explored the dose ranges over which the different clearance mechanisms predominate.

METHODS

Animals

The animal studies were approved by The University of Melbourne Animal Experimentation Ethics Committee and were conducted in accordance with the National Institutes of Health "Guidelines for the Care and Use of Laboratory Animals". Adult merino wether sheep weighing between 41 and 69 kg were supplied by the Victorian Institute of Animal Science (Werribee, Australia). During the pharmacokinetic studies sheep were housed in metabolism cages and food and water were available *ad libitum*.

Experimental Procedures

A parallel study design was selected to explore the pharmacokinetics of rhLIF after IV and SC administration. Six groups of two sheep each received a single IV bolus rhLIF dose of 12.5, 25, 100, 250, 500 or 750 µg/kg into the jugular vein. Three groups of four sheep received SC rhLIF injected into the inter-digital space of the hind leg at a single dose of 10, 20 or 50 µg/kg. All animals had a 16 gauge, 133 mm Angiocath™ IV catheter (Becton Dickinson, Utah) inserted into the jugular vein (contralateral to that used for IV injection) to facilitate sampling of systemic blood.

Formulation of rhLIF

Recombinant human LIF was provided by Amrad Corporation Ltd (Melbourne, Australia) as a stock solution containing 2.78 or 3.08 mg/mL rhLIF in 2 mM phosphate buffer. Undiluted stock solution was used to administer IV doses of 100, 250, 500 and 750 µg/kg rhLIF. Dosing solutions for the IV administration of 12.5 or 25 µg/kg doses were prepared by diluting rhLIF stock solution 5- or 3-fold, respectively, with 2 mM phosphate buffer. This dilution was necessary to provide an adequate volume to accurately draw up and inject. For SC administration, doses were formulated as neutral,

isotonic solutions with a constant dosing volume of 1.5 mL. The concentration of rhLIF in the formulations for SC injection varied from 0.3 to 1.6 mg/mL depending on the dose administered and the weight of the individual sheep. Dilutions and formulation adjustments were conducted on the morning of the study, and all dosing solutions were sterile filtered through a 0.22 µm Millex®-GV syringe filter (Millipore, Bedford, MA) immediately prior to administration.

Sample Collection

Pre-dosing blood samples were collected from each animal immediately prior to rhLIF administration. After IV injection, blood samples were withdrawn via the in-dwelling jugular vein catheter at 1, 3, 6, 15, 30, and 45 min, 1, 1.5, 2, 2.5, and 3 h, then the sampling continued at 2-3 hourly intervals depending on the dose administered. The total number of sample time points ranged from 10 to 23, corresponding to the lowest and highest IV doses, respectively. When rhLIF was given by the SC route, blood samples were withdrawn at 0.5, 1, 1.5, 2, 2.5, 3, 4, 5, 6, 8, 10 and 12 h post-dosing. Two mL of blood was initially withdrawn and discarded to flush the catheter and ensure the collection of circulating blood. A subsequent 3 mL sample of blood was withdrawn and transferred to di-potassium EDTA tubes (Sarstedt, Australia). Blood samples were centrifuged at 3000 rpm for 10 min then the plasma was separated and frozen at -20°C until analysis. Between periods of sampling the jugular vein catheters were kept patent with a heparin saline flush (10 IU/mL).

Sample Analysis

Plasma samples were analyzed for immunoreactive rhLIF using a commercially available ELISA for recombinant human LIF (Quantikine™, R&D Systems, Minneapolis, MN). The ELISA was performed according to the manufacturer's instructions and was

validated for use with a sheep plasma matrix. Analysis of pre-dosing sheep plasma samples indicated the absence of cross-reacting species. Comparison of triplicate spiked plasma samples (50, 500 and 2000 pg/mL) to a calibration curve (31-2000 pg/mL) analysed in one assay and repeated on three different days, indicated that intra- and inter-assay precision were less than 15%. The measured concentrations of the spiked plasma samples assessed by back-calculation relative to the calibration curve were within 15% of the nominal concentrations. The limit of quantitation (LOQ) for the assay was defined as the lowest spiked plasma sample (50 pg/mL) that demonstrated acceptable accuracy and precision (<15%). Samples containing rhLIF at concentrations above the ELISA calibration range (2000 pg/mL) were diluted with blank pooled sheep plasma prior to analysis.

Non-compartmental Pharmacokinetic Analysis

Non-compartmental analysis of rhLIF pharmacokinetics was performed using WinNonlin™ Professional Version 3.2 (Pharsight Corporation, Mountain View, CA). Individual plasma concentrations and sample times for each animal were used in the analysis. For IV administration of rhLIF, the initial plasma concentration (C_p^0), initial distribution volume (V_c), terminal slope (λ), terminal elimination half-life ($t_{1/2}$), total area under the plasma concentration-time curve extrapolated to infinity (AUC), systemic plasma clearance (CL), and steady-state volume of distribution (V_{ss}) were calculated by standard methods (Gibaldi and Perrier, 1992). Following SC administration of rhLIF, the peak plasma concentration (C_{max}) and the time to C_{max} (T_{max}) were taken directly from individual profiles. The terminal slope, $t_{1/2}$ and AUC were calculated by standard methods as for IV dosing.

Statistical analysis of the calculated non-compartmental parameters was conducted using a standard statistical software package (Sigmastat™, Jandel Scientific, CA). Differences were considered significant at $p<0.05$. For the SC groups, statistical comparisons of the dose-normalized AUC and $t_{1/2}$ were conducted using a one-way ANOVA with Tukey's multiple comparisons. Statistical comparisons for T_{max} were conducted using a Kruskal-Wallis one-way ANOVA on ranks.

Pharmacokinetic Model for rhLIF

Based on the physicochemical properties of rhLIF and the common absorption and clearance pathways for protein drugs, a mechanistic model was proposed to describe the pharmacokinetics of rhLIF after IV and SC administration (Figure 1). The model for rhLIF was based on a generalised pharmacokinetic model for drugs exhibiting target-mediated drug disposition (TMDD) as originally described by Mager and Jusko (2001). This generalised model has successfully been applied to describe the pharmacokinetics of several recombinant cytokines including interferon-β 1a (Mager et al., 2003), vascular endothelial growth factor (Eppler et al., 2002) and thrombopoietin (Jin and Krzyzanski, 2002). The key feature of the model, and that which imparts nonlinearity to the distribution and elimination kinetics, is high affinity, saturable binding of rhLIF to specific pharmacological receptors on cell surfaces and subsequent internalization and degradation of the entire rhLIF-receptor complex. *In vitro* studies have demonstrated that LIF displays typical cytokine binding kinetics characterized by a rapid rate of binding and a slow dissociation rate, with an average reported equilibrium dissociation constant (K_d) of approximately 0.1 nM (Hilton et al., 1988; Godard et al., 1992; Tomida, 2000). As the density of high affinity receptors on LIF responsive cells is relatively low, with an

average of 300 binding sites per cell (Godard et al., 1992; Tomida, 2000), LIF binding is a low capacity process that may readily become saturated. Following receptor binding, the entire LIF-receptor complex is subject to internalization and degradation by lysosomal enzymes (Bower et al., 1995).

In the proposed model, rhLIF enters the systemic circulation (central compartment; A_P, V_c) directly following IV bolus administration or is absorbed from the interstitium following SC injection (the absorption model is discussed below). Circulating rhLIF binds to pharmacological receptors (R) to form rhLIF-receptor complexes (RC) as described by the second-order association rate constant, k_{on}. The initial quantity of receptors (R_m) is modeled as a parameter and is allowed to vary for different dose levels to account for receptor up- or down-regulation. Unoccupied LIF receptors are subject to a constant turnover governed by a zero-order production rate (k_{syn}) and a first-order rate of degradation (k_{deg}). Following binding, the model allows for dissociation of rhLIF from the receptor according to a first-order dissociation rate constant, k_{off}, or for the internalization of the entire rhLIF-receptor complex and degradation by lysosomal enzymes. The collective processes of internalization, intra-cellular transport and lysosomal degradation are characterized by a first-order rate constant, k_{int}. As *in vitro* studies have demonstrated that the LIF receptor is degraded within the cell, a receptor recycling component is not required in this model (Bower et al., 1995).

In addition to clearance by receptor-mediated endocytosis, rhLIF is also likely to be subject to renal elimination as is common for proteins with a molecular weight below that of albumin (67 kDa) (Maack et al., 1979). Non-specific degradation by circulating proteases or hepatic catabolism are further potential mechanisms for the clearance of rhLIF (Ferraiolo et al., 1992). These non-specific, high-capacity elimination processes

JPET Fast Forward. Published on February 10, 2004 as DOI: 10.1124/jpet.103.063289
This article has not been copyedited and formatted. The final version may differ from this version.

are included in the proposed model as a single first-order elimination process from the central compartment (k_e). The model also includes first-order transfer of rhLIF between the central compartment (A_P) and a tissue compartment (A_T) to account for extravascular distribution and/or non-specific drug binding. Initially, the inter-compartmental distribution rate constants were estimated as separate parameters, however the estimates were consistently similar and were subsequently fixed to be equal (k_{nsb}) thus reducing the number of parameters in the model.

The SC absorption of rhLIF was modeled as a first-order input process into an absorption delay compartment (A_D; k_{a1}) and subsequent first-order transfer into the systemic circulation (A_P; k_{a2}). The delay compartment was included to reflect diffusion of rhLIF through the interstitium, reversible binding at the injection site and/or possible transport of rhLIF through the lymphatic system. The first-order rate of transfer from the absorption delay compartment into the systemic circulation (k_{a2}) was allowed to vary with dose to account for dose-dependency in the absorption process. The bioavailability of rhLIF was initially modeled as a parameter, however preliminary analysis indicated that the bioavailability was consistently estimated as close to 100%, and was therefore fixed to this value (data not shown).

The system can be defined by the following differential equations:

$$\frac{dA_{P(IV)}}{dt} = k_{nsb} \cdot A_T - (k_{nsb} + k_e) \cdot A_P - \left(\frac{k_{on}}{V_c}\right) \cdot A_P \cdot R + k_{off} \cdot RC \qquad (1)$$

$$\frac{dA_{P(SC)}}{dt} = k_{a2} \cdot A_D + k_{nsb} \cdot A_T - (k_{nsb} + k_e) \cdot A_P - \left(\frac{k_{on}}{V_c}\right) \cdot A_P \cdot R + k_{off} \cdot RC \qquad (2)$$

JPET Fast Forward. Published on February 10, 2004 as DOI: 10.1124/jpet.103.063289
This article has not been copyedited and formatted. The final version may differ from this version.

$$\frac{dA_T}{dt} = k_{nsb} \cdot (A_P - A_T) \quad (3)$$

$$\frac{dRC}{dt} = \left(\frac{k_{on}}{V_c}\right) \cdot A_P \cdot R - (k_{off} + k_{int}) \cdot RC \quad (4)$$

$$\frac{dR}{dt} = k_{syn} - \left(\frac{k_{on}}{V_c}\right) \cdot A_P \cdot R + k_{off} \cdot RC - k_{deg} \cdot R \quad (5)$$

$$\frac{dA_{D(SC)}}{dt} = k_{a1} \cdot D_{SC} \cdot e^{(-k_{a1} \cdot t)} - k_{a2} \cdot A_D \quad (6)$$

where equations 1, 3, 4 and 5 describe the disposition of rhLIF following IV administration and equations 2, 3, 4, 5 and 6 describe the absorption and disposition of rhLIF administered by SC injection. The amounts of rhLIF and receptor in the above equations were modeled in units of nanomoles per kilogram, and the rhLIF plasma concentrations were estimated as A_P/V_c with conversion to units of nanogram per millilitre. The symbols used in the equations are defined in the abbreviation list.

The proposed pharmacokinetic model was simultaneously fitted to the mean plasma drug concentrations for both the IV and SC routes of administration and all dose levels to obtain a single set of parameters to characterize the entire data set. The parameters estimated included k_{a1}, k_{a2}, k_{nsb}, k_e, k_{deg}, k_{on}, k_{int}, R_m and V_c. The values for k_{syn} and k_{off} were determined as secondary parameters according to the relationships $k_{syn} = k_{deg} \cdot R_m$ and $k_{off} = k_{on} \cdot K_d$, respectively. Initially both k_{on} and k_{off} were estimated, providing a calculated K_d value that was similar to the mean reported literature value of 0.1 nM (Hilton et al., 1988; Godard et al., 1992; Tomida, 2000), and thus K_d was fixed during the modelling process to reduce the number of parameters to be estimated. Initial parameter estimates were derived from the characteristics of the observed plasma

JPET Fast Forward. Published on February 10, 2004 as DOI: 10.1124/jpet.103.063289
This article has not been copyedited and formatted. The final version may differ from this version.

concentration-time profiles as previously described for compounds demonstrating target-mediated drug disposition (Mager and Jusko, 2001). Parameters were estimated using the ADAPT II software (D'Argenio and Schumitzky, 1997) by the maximum likelihood method. The variance model was defined as follows:

$$VAR_i = \sigma_1^2 \cdot M(\theta, t_i)^{\sigma_2} \qquad (7)$$

where VAR_i is the variance of the i^{th} data point, σ_1 and σ_2 are the variance parameters (σ_2=2), and $M(\theta,t_i)$ is the i^{th} predicted value from the pharmacokinetic model. Using the final parameter estimates, computer simulations were performed to generate profiles of the fraction of receptors involved in binding as a function of time.

The goodness of fit was assessed by model convergence, visual inspection, examination of the residuals, precision of the parameter estimates, Akaike Information Criteria (AIC), Schwarz Criterion (SC) and the estimator criterion value for the maximum likelihood method in ADAPT II.

RESULTS

Non-compartmental Pharmacokinetic Analysis

The mean plasma concentration-time profiles following IV and SC administration of a wide range of rhLIF doses to sheep are shown in Figure 2. Administration of the lower IV doses resulted in a rapid decline in plasma concentrations, whereas higher rhLIF doses produced more complex profiles characterized by regions of convexity and increasingly prolonged terminal phase half-lives. By visual inspection, the time required to reach the maximum plasma concentration after SC administration of rhLIF appeared to be prolonged for the lower dose levels, and the peak concentration was followed by an apparent mono-exponential decline in plasma concentrations.

Table 1 reports the average (n=2) pharmacokinetic parameters obtained by non-compartmental analysis following IV administration of rhLIF. There was minimal variability between the two sheep at each IV dose level, with individual pharmacokinetic parameters generally differing by less than 20% from average values. Table 2 summarises the mean parameter estimates (n=4) generated by non-compartmental analysis of individual SC profiles. Following IV administration, an increase in dose generally resulted in a proportional increase in Cp^0. There were however, slight departures from linearity at the two lowest doses where less than proportional increases in Cp^0 were evident. Consistent with this trend, V_c was relatively consistent across the four highest IV dose levels, with a mean value of approximately 38 mL/kg, but again there were deviations at the two lower doses of 12.5 and 25 µg/kg where the calculated values for V_c were 69 and 51 mL/kg, respectively. The AUC increased with IV dose in a greater than proportional manner, with a 10-fold increase in dose (from 25 to 250 µg/kg) resulting in a 15-fold increase in AUC, and there was a corresponding dose-dependent

decrease in systemic plasma clearance. V_{ss} was variable over the rhLIF dose range investigated, but was consistently larger than the volume of the central compartment.

Following SC administration, the time to reach the maximum plasma concentration (T_{max}) was variable, with individual values ranging from 1 to 6 hours (Table 2). Although the median T_{max} appeared to be prolonged at lower doses, statistical analysis revealed no significant difference. Both C_{max} and AUC increased in a greater than proportional manner with dose, with a 5-fold increase in SC dose resulting in a 35-fold increase in AUC and a 60-fold increase in C_{max}. The dose-normalized values for AUC and C_{max} were statistically different between dosing levels. The terminal half-lives were not statistically different across the three SC dose levels but were longer than those observed following IV administration presumably reflecting a slow rate of rhLIF absorption from the injection site (flip-flip pharmacokinetics).

Pharmacokinetic Model

The pharmacokinetic profiles generated by simultaneously fitting the data after both IV and SC administration to the proposed model (Figure 1) are shown in Figure 2. The model captured the pharmacokinetic data relatively well for all doses and both routes of administration, although there were slight over-estimations of the observed plasma concentrations following administration of the lower IV dose levels. The final model parameters were estimated with good precision, with all but one parameter showing CV% values less than 23% (Table 3). The variance model parameter (σ_1 in Equation 7) was estimated as 0.35 (6.8 CV%). The estimated volume of the central compartment was 53 mL/kg which is slightly larger than the physiological plasma volume reported for sheep of 39 mL/kg (Adams and McKinley, 1995). Adequate model fitting

JPET Fast Forward. Published on February 10, 2004 as DOI: 10.1124/jpet.103.063289
This article has not been copyedited and formatted. The final version may differ from this version.

necessitated the initial quantity of LIF receptors to vary for the highest IV rhLIF dosing level (750 µg/kg), designated R_m'. The estimated degradation rate of free receptor (0.566 h^{-1}) was approximately four times slower than the rate of internalization and degradation of the rhLIF-receptor complex (2.047 h^{-1}). This finding is in agreement with an *in vitro* study conducted using murine cells that indicated that unoccupied (free) receptors were internalised or degraded more slowly (0.42 h^{-1}) than occupied receptors (1.86 h^{-1}) (Hilton and Nicola, 1992).

When rhLIF was administered subcutaneously, the first-order rate of rhLIF transfer from the SC injection site into the absorption delay compartment (k_{a1}) was assumed to be the rate limiting step and was estimated as a single value for all three dose levels. An optimal fit of the SC data required that the subsequent rate constant describing transfer of rhLIF from the delay compartment into the systemic circulation (k_{a2}) be a different value for each SC dose. It is important to note that the absorption rate constants, k_{a1} and k_{a2}, are not uniquely identifiable and further studies would be required to determine which is the rate-limiting step for absorption. As a previous study had indicated that a binding protein for LIF may be present in the extracellular matrix (Mereau et al., 1993), a saturable binding process at the SC injection site was included in the model in an attempt to enhance the physiological relevance. Inclusion of this additional element, however, resulted in over-parameterization of the model, given the limited data available (data not shown).

To ensure that all compartments and elimination processes were necessary to adequately describe the disposition of rhLIF, the proposed model was simplified by sequentially excluding either first-order elimination from the central compartment (k_e), non-specific binding (k_{nsb}) or internalization and degradation of the rhLIF-receptor

JPET Fast Forward. Published on February 10, 2004 as DOI: 10.1124/jpet.103.063289
This article has not been copyedited and formatted. The final version may differ from this version.

complex (k_{int}). In all cases, model simplification resulted in unstable fitting and visually poor fits indicating that all model components were required (data not shown).

DISCUSSION

The pharmacokinetics of recombinant cytokines are inherently complex and frequently demonstrate nonlinearity (Piscitelli et al., 1997). Consequently, comprehensive studies are required to fully characterise the *in vivo* behaviour of cytokines to enable accurate prediction of their pharmacokinetic properties and facilitate the design of rational dose regimens. The objective of the present study was to assess the pharmacokinetics of rhLIF over a wide range of doses administered intravenously and subcutaneously to sheep. In the first instance, the pharmacokinetics were evaluated by non-compartmental analysis. Subsequently, a physiologically relevant, mechanistic model was developed to characterise the kinetic behaviour.

Administration of rhLIF by IV bolus injection resulted in plasma concentration-time profiles showing trends towards more prominent initial distribution phases, enhanced convexity and prolonged terminal elimination phases with increasing dose. Non-compartmental analysis revealed a disproportionate increase in AUC and a corresponding decrease in plasma clearance with increasing dose, confirming the existence of nonlinear pharmacokinetics. The clearance of rhLIF was extremely rapid, particularly at the lowest IV dose (12.5 µg/kg) where the systemic clearance was 5.2 mL/min/kg. Renal filtration is often considered to be a major clearance pathway for proteins with molecular weights below that of albumin, with the process being most efficient for proteins smaller than 30 kDa (Maack et al., 1979). With rhLIF, however, renal filtration is unlikely to be the predominant mechanism given that the total clearance at low doses far exceeds the glomerular filtration rate in sheep (1.2 mL/min/kg: (Adams and McKinley, 1995)). It is therefore evident that additional elimination mechanisms must contribute to the systemic clearance of rhLIF.

Given the nonlinear disposition of rhLIF, traditional models of monophasic or biphasic exponential decline were unsuitable to describe the plasma pharmacokinetics across all dose levels, and therefore a model has been suggested based on the pharmacology of rhLIF and knowledge of the common clearance mechanisms for protein drugs (Figure 1). In this model, the predominant clearance pathway was high affinity binding of rhLIF to specific cell-surface receptors followed by endocytosis and degradation. Considering the complexity of the plasma concentration-time profiles, the proposed model well characterized the pharmacokinetics of rhLIF across the wide range of doses and both IV and SC routes of administration.

While target-mediated drug disposition and degradation following endocytosis are the key features of the model, adequate characterization of rhLIF disposition required the inclusion of a parallel first-order elimination process from the central compartment which most likely reflects renal elimination. The relative significance of the linear elimination pathway can be assessed by comparison of the model predicted clearance via first-order elimination ($k_e \cdot V_c$) of 1.37 mL/min/kg to the apparent total plasma clearance obtained for each dose by non-compartmental analysis of the IV data (Table 1). As the dose of rhLIF increases, the linear elimination pathway becomes increasingly important because clearance via receptor mediated endocytosis is saturated. For example, clearance via the first-order process for the 12.5, 100 and 500 µg/kg rhLIF doses constitutes 26, 60 and 90% of the total clearance of rhLIF, respectively. A further model component that was found to be necessary to adequately characterize the disposition of rhLIF was the reversible transfer of rhLIF between the central compartment and a tissue compartment (A_T). This tissue compartment could

represent extravascular distribution of rhLIF, or alternatively, could reflect non-specific binding of rhLIF to plasma proteins such as α_1-acid glycoprotein or α_2-macroglobulin.

Optimal characterization of rhLIF kinetics with the present model necessitated that R_m be a lower value for the highest IV dose (750 µg/kg). Without this provision, the model systematically over-estimated the observed plasma concentration-time profile following administration of 750 µg/kg rhLIF (data not shown). It is proposed that the pharmacokinetic behaviour of rhLIF after administration of very high doses could be altered as a consequence of receptor down-regulation. This proposal is supported by *in vitro* studies using various cell types that indicated autologous regulation of the LIF receptor within 2 hours following treatment with LIF (Bower et al., 1995; Blanchard et al., 2000). Inclusion of a receptor down-regulation process into the current model was not feasible without additional experimental data such as receptor concentrations or supporting pharmacodynamic data. As an alternative, the empirical approach of allowing R_m to be a lower value for the highest rhLIF IV dose was adopted and resulted in predicted profiles that better reflected the observed pharmacokinetic data with the addition of only one extra model parameter.

The utility of employing a lower R_m value to reflect receptor down-regulation can be appreciated by examining the predicted changes in free receptor density over time. In Figure 3, the free receptor density was simulated for a range of rhLIF doses using the parameter estimates for the final model (Table 3). An extremely rapid initial decline in receptor density is apparent after IV administration reflecting the high-affinity binding of rhLIF to the available cell-surface receptors. Synthesis of new receptor and dissociation of the rhLIF-receptor complex resulted in a subsequent gradual rise in free receptor

density. For the 750 µg/kg rhLIF dose, where R_m' was estimated as 0.058 nmol/kg, the receptor densities remained at low levels for a sustained period of time, such that even 24 hours after dosing the receptor density had not returned to initial levels.

Although saturable target-mediated drug disposition appeared to adequately describe the plasma concentration-time data in the present study, it is possible that an additional nonlinear binding process could also contribute to the highly complex disposition of rhLIF, since the observed relationship between the administered dose and V_{ss} (Table 1) was not typical of target-mediated drug disposition. For drugs that bind with high affinity to their pharmacological targets, V_{ss} generally decreases with increasing dose to approach plasma volume (Levy, 1994). This has been observed previously with several protein-based drugs including IFN-β1a and natalizumab (Sheremata et al., 1999; Mager et al., 2003). However, if an additional saturable binding protein, such as a soluble LIF receptor (which has previously been identified in human plasma (Zhang et al., 1998)), was present in sheep plasma, the outcome is less certain and changes in V_{ss} are difficult to predict.

The development of a model to describe the absorption kinetics of rhLIF following SC administration was confounded by the nonlinear disposition, flip-flop kinetics and poorly defined absorption mechanisms. Initially, a wide range of absorption models including single zero- and first-order absorption processes, and combinations of zero- and first-order input occurring in parallel or sequentially and with or without lag times, were evaluated for their ability to characterize the absorption of rhLIF. The absorption process was best described by first-order input into a delay compartment, and subsequent first-order transfer to the systemic circulation. This model likely reflects the slow transport of the relatively large sized rhLIF through the interstitium, a process which

may be further hindered by the interaction of highly basic rhLIF (pI 9.15) with negatively-charged interstitial glycosaminoglycans. The slow rate of absorption of subcutaneously administered proteins has also been attributed to uptake into and transport through the lymphatic system (Radwanski et al., 1998). Several studies have quantitatively demonstrated that the lymphatics are the primary absorption pathway for proteins with a molecular weight above 16 kDa (Supersaxo et al., 1990; Charman et al., 2000; McLennan et al., 2003), and it is therefore expected that this pathway would contribute to the absorption of subcutaneously administered rhLIF (19.71 kDa). The data in the current study are not sufficiently rich to delineate the relative contributions of interstitial transfer and lymphatic transport to the absorption kinetics of rhLIF, however, studies are currently underway to investigate the rate and extent of rhLIF lymphatic transport which will provide a greater understanding of the underlying absorption mechanisms for this protein.

In the SC model, the estimate for k_{a1} was fixed to be equal for all three dose levels, however, the rate constant for transfer of rhLIF from the absorption delay compartment to the systemic circulation (k_{a2}) was best modeled as a different value for each of the SC doses to capture the apparent differences in the time to reach C_{max}. Although definitive evidence is lacking, a possible explanation for the quicker absorption with the higher rhLIF doses is that the higher protein concentration in the formulation (note that injection volumes were constant for all SC dose levels) increased the oncotic pressure in the interstitium promoting interstitial transport and/or lymphatic filling.

In summary, the current study is the first to comprehensively examine the dose-proportionality of rhLIF pharmacokinetics, and has demonstrated that the pharmacokinetics of rhLIF in sheep are complex and significantly nonlinear following

both IV and SC administration. The nonlinear disposition was successfully characterised using a model that featured specific binding of rhLIF to high-affinity, low-capacity cell-surface receptors, followed by internalization and degradation of the rhLIF-receptor complex. The apparent time course of receptor occupancy predicted by the model could potentially be used as a basis for future pharmacodynamic models of rhLIF pharmacological effects, and in more general terms, the results further support the relevance of this pharmacokinetic model for cytokines and protein drugs where the specific site of action also acts as a clearance pathway.

REFERENCES

Adams D and McKinley M (1995) The Sheep. *Anzccart News* **8**:1-4.

Blanchard F, Duplomb L, Wang Y, Robledo O, Kinzie E, Pitard V, Godard A, Jacques Y and Baumann H (2000) Stimulation of leukemia inhibitory factor receptor degradation by extracellular signal-regulated kinase. *J Biol Chem* **275**:28793-28801.

Bower J, Vakakis N, Nicola NA and Austin L (1995) Specific binding of leukemia inhibitory factor to murine myoblasts in culture. *J Cell Physiol* **164**:93-98.

Chapel SH, Veng-Pedersen P, Schmidt RL and Widness JA (2001) Receptor-based model accounts for phlebotomy-induced changes in erythropoietin pharmacokinetics. *Exp Hematol* **29**:425-431.

Charman SA, Segrave AM, Edwards GA and Porter CJ (2000) Systemic availability and lymphatic transport of human growth hormone administered by subcutaneous injection. *J Pharm Sci* **89**:168-177.

D'Argenio DZ and Schumitzky A (1997) *ADAPT II User's Guide: Pharmacokinetic / Pharmacodynamic Systems Analysis Software*. Biomedical Simulations Resource, Los Angeles.

Eppler SM, Combs DL, Henry TD, Lopez JJ, Ellis SG, Yi JH, Annex BH, McCluskey ER and Zioncheck TF (2002) A target-mediated model to describe the pharmacokinetics and hemodynamic effects of recombinant human vascular endothelial growth factor in humans. *Clin Pharmacol Ther* **72**:20-32.

Ferraiolo BL, Mohler MA and Gloff CA (1992) *Protein Pharmacokinetics and Metabolism*. Plenum Press, New York.

Gearing DP, Comeau MR, Friend DJ, Gimpel SD, Thut CJ, McGourty J, Brasher KK, King JA, Gillis S, Mosley B, Ziegler SF and Cosman D (1992) The IL-6 signal transducer, gp130: an oncostatin M receptor and affinity converter for the LIF receptor. *Science* **255**:1434-1437.

Gearing DP, Gough NM, King JA, Hilton DJ, Nicola NA, Simpson RJ, Nice EC, Kelso A and Metcalf D (1987) Molecular cloning and expression of cDNA encoding a murine myeloid leukaemia inhibitory factor (LIF). *EMBO J* **6**:3995-4002.

Gibaldi M and Perrier D (1992) *Pharmacokinetics*. Marcel Dekker, New York.

Godard A, Heymann D, Raher S, Anegon I, Peyrat MA, Le Mauff B, Mouray E, Gregoire M, Virdee K, Soulillou JP, Moreau F and Jacques Y (1992) High and low affinity receptors for human interleukin for DA cells/leukemia inhibitory factor on human cells. Molecular characterization and cellular distribution. *J Biol Chem* **267**:3214-3222.

Gunawardana DH, Basser RL, Davis ID, Cebon J, Mitchell P, Underhill C, Kilpatrick TJ, Reardon K, Green MD, Bardy P, Amor P, Crump D, Ng S, Nation RL and Begley CG (2003) A phase I study of recombinant human leukemia inhibitory factor in patients with advanced cancer. *Clinical Cancer Research* **9**:2056-2065.

Hilton DJ (1992) LIF: lots of interesting functions. *Trends Biochem Sci* **17**:72-76.

Hilton DJ and Gough NM (1991a) Leukemia inhibitory factor: a biological perspective. *J Cell Biochem* **46**:21-26.

Hilton DJ and Nicola NA (1992) Kinetic analyses of the binding of leukemia inhibitory factor to receptors on cells and membranes and in detergent solution. *J Biol Chem* **267**:10238-10247.

Hilton DJ, Nicola NA and Metcalf D (1988) Specific binding of murine leukemia inhibitory factor to normal and leukemic monocytic cells. *Proc Natl Acad Sci USA* **85**:5971-5975.

Hilton DJ, Nicola NA, Waring PM and Metcalf D (1991b) Clearance and fate of leukemia-inhibitory factor (LIF) after injection into mice. *J Cell Physiol* **148**:430-439.

Jin F and Krzyzanski W (2002) Pharmacokinetic model of target-mediated disposition of thrombopoietin. *AAPS Pharm Sci* **4**: W5238.

Kurek J (2000) AM424: history of a novel drug candidate. *Clin Exp Pharmacol Physiol* **27**:553-557.

Levy G (1994) Pharmacologic target-mediated drug disposition. *Clin Pharmacol Ther* **56**:248-252.

Liu KX, Kato Y, Terasaki T, Aoki S, Okumura K, Nakamura T and Sugiyama Y (1995) Contribution of parenchymal and non-parenchymal liver cells to the clearance of hepatocyte growth factor from the circulation in rats. *Pharm Res* **12**:1737-1740.

Maack T, Johnson V, Kau ST, Figueiredo J and Sigulem D (1979) Renal filtration, transport, and metabolism of low-molecular-weight proteins: a review. *Kidney Int* **16**:251-270.

Mager DE and Jusko WJ (2001) General pharmacokinetic model for drugs exhibiting target-mediated drug disposition. *J Pharmacokinet Pharmacodyn* **28**:507-532.

Mager DE, Neuteboom B, Efthymiopoulos C, Munafo A and Jusko WJ (2003) Receptor-mediated pharmacokinetics and pharmacodynamics of interferon-beta1a in monkeys. *J Pharmacol Exp Ther* **306**:262-270.

McLennan DN, Porter CJH, Edwards GA, Brumm M, Martin SW and Charman SA (2003) Pharmacokinetic model to describe the lymphatic absorption of r-met-Hu-Leptin after subcutaneous injection to sheep. *Pharm Res* **20**:1156-1162.

Mereau A, Grey L, Piquet-Pellorce C and Heath JK (1993) Characterization of a binding protein for leukemia inhibitory factor localized in extracellular matrix. *J Cell Biol* **122**:713-719.

Piscitelli SC, Reiss WG, Figg WD and Petros WP (1997) Pharmacokinetic studies with recombinant cytokines. Scientific issues and practical considerations. *Clin Pharmacokinet* **32**:368-381.

Radwanski E, Chakraborty A, Van Wart S, Huhn RD, Cutler DL, Affrime MB and Jusko WJ (1998) Pharmacokinetics and leukocyte responses of recombinant human interleukin-10. *Pharm Res* **15**:1895-1901.

Sheremata WA, Vollmer TL, Stone LA, Willmer-Hulme AJ and Koller M (1999) A safety and pharmacokinetic study of intravenous natalizumab in patients with MS. *Neurology* **52**:1072-1074.

Stewart CL, Kaspar P, Brunet LJ, Bhatt H, Gadi I, Kontgen F and Abbondanzo SJ (1992) Blastocyst implantation depends on maternal expression of leukaemia inhibitory factor. *Nature* **359**:76-79.

Sugiyama Y and Hanano M (1989) Receptor-mediated transport of peptide hormones and its importance in the overall hormone disposition in the body. *Pharm Res* **6**:192-202.

Supersaxo A, Hein WR and Steffen H (1990) Effect of molecular weight on the lymphatic absorption of water-soluble compounds following subcutaneous administration. *Pharm Res* **7**:167-169.

Terashi K, Oka M, Ohdo S, Furukubo T, Ikeda C, Fukuda M, Soda H, Higuchi S and Kohno S (1999) Close association between clearance of recombinant human granulocyte colony-stimulating factor (G-CSF) and G-CSF receptor on neutrophils in cancer patients. *Antimicrob Agents Chemother* **43**:21-24.

Tomida M (2000) Structural and functional studies on the leukemia inhibitory factor receptor (LIF-R): gene and soluble form of LIF-R, and cytoplasmic domain of LIF-R required for differentiation and growth arrest of myeloid leukemic cells. *Leukemia & Lymphoma* **37**:517-525.

Waring P (1997) Leukemia Inhibitory Factor, in *Colony-Stimulating Factors : Molecular and Cellular Biology* (Garland JM, Quesenberry PJ and Hilton DJ eds) pp 467-513, Marcel Dekker, New York.

Williams RL, Hilton DJ, Pease S, Willson TA, Stewart CL, Gearing DP, Wagner EF, Metcalf D, Nicola NA and Gough NM (1988) Myeloid leukaemia inhibitory factor maintains the developmental potential of embryonic stem cells. *Nature* **336**:684-687.

Willson TA, Metcalf D and Gough NM (1992) Cross-species comparison of the sequence of the leukaemia inhibitory factor gene and its protein. *Eur J Biochem* **204**:21-30.

Yamamoto-Yamaguchi Y, Tomida M and Hozumi M (1992) Prolongation by differentiation-stimulating factor/leukemia inhibitory factor of the survival time of mice implanted with mouse myeloid leukemia cells. *Leuk Res* **16**:1025-1029.

Zhang JG, Zhang Y, Owczarek CM, Ward LD, Moritz RL, Simpson RJ, Yasukawa K and Nicola NA (1998) Identification and characterization of two distinct truncated forms of gp130 and a soluble form of leukemia inhibitory factor receptor alpha-chain in normal human urine and plasma. *J Biol Chem* **273**:10798-10805.

FOOTNOTES

*Authors contributed equally to this publication

This work was funded by Amrad Corporation Limited and the Intramural Research Program of the National Institute on Aging.

LEGENDS FOR FIGURES

Figure 1.

Proposed pharmacokinetic model for rhLIF administered by IV or SC bolus injection. The key feature of the model is target-mediated drug disposition where rhLIF binds to specific receptors on cell surfaces (k_{on}) to form rhLIF-receptor complexes (RC). rhLIF can dissociate from the receptor (k_{off}) or the rhLIF-receptor complex can be internalized into the cell and degraded (k_{int}). Free receptor (R) is subject to constant turnover characterized by a zero-order production rate constant (k_{syn}) and a first-order degradation rate constant (k_{deg}). rhLIF can also participate in reversible linear non-specific binding (k_{nsb}) or be eliminated by first-order processes from the central compartment (k_e).

Figure 2.

Plasma concentration-time profiles of rhLIF following IV (Panel A) or SC (Panel B) administration. The lines represent the predicted profiles when the proposed model (Figure 1) was simultaneously fit to the observed mean data for all dose levels and both routes of administration. IV doses are 12.5 (●), 25 (○), 100 (▼), 250 (▽), 500 (■), and 750 (□) µg/kg rhLIF. SC doses are 10 (▲), 20 (△) and 50 (◆) µg/kg rhLIF. Error bars represent the standard error of the mean.

Figure 3.

Simulation of the free receptor density available for rhLIF binding over time (R in Equation 5) following IV administration of a range of rhLIF doses using the proposed model (Figure 1) and the final parameter estimates (Table 3). Data are expressed as the

proportion of the initial receptor density (R_m or R_m'). Note the immediate initial rapid decline in free receptor density as rhLIF is rapidly acquired by specific cell-surface receptors.

JPET Fast Forward. Published on February 10, 2004 as DOI: 10.1124/jpet.103.063289
This article has not been copyedited and formatted. The final version may differ from this version.

TABLE 1

Pharmacokinetic parameters determined by non-compartmental analysis following IV administration of a range of rhLIF doses.[a]

Dose (μg/kg)	Cp^0 (ng/mL)	V_c (mL/kg)	AUC (ng·h/mL)	CL (mL/min/kg)	V_{ss} (mL/kg)	$t_{1/2}$ (h)
12.5	181	68.9	41.5	5.18	90.9	0.27
25	501	50.9	152	2.76	60.1	0.33
100	2572	39.0	735	2.30	58.3	0.82
250	6879	36.9	2254	1.85	76.2	1.16
500	13248	37.7	5474	1.53	70.1	2.03
750	19209	39.1	11592	1.09	81.0	2.29

[a] Values reported are the average for two animals

JPET Fast Forward. Published on February 10, 2004 as DOI: 10.1124/jpet.103.063289
This article has not been copyedited and formatted. The final version may differ from this version.

TABLE 2

Pharmacokinetic parameters determined for individual animals administered SC rhLIF by non-compartmental analysis.

Dose (μg/kg)	C_{max}[a] (ng/mL)	T_{max}[b] (h)	AUC[a] (ng·h/mL)	$t_{1/2}$[a] (h)
10	1.02	3.75	5.36	1.79
	(0.16)	[1.5-6.0]	(0.5)	(0.16)
20	9.79	2.5	27.8	1.81
	(0.53)	[1.0-3.0]	(3.77)	(0.25)
50	61.9	1.75	187	1.26
	(6.94)	[1.0-2.0]	(32.8)	(0.06)

[a] Values are reported as mean (standard error)

[b] Values are reported as median [range]

JPET Fast Forward. Published on February 10, 2004 as DOI: 10.1124/jpet.103.063289
This article has not been copyedited and formatted. The final version may differ from this version.

TABLE 3

Final estimated model parameters of rhLIF pharmacokinetics in sheep.

Parameter (units)	Final estimate	CV (%)
k_{nsb} (h^{-1})	0.338	4.6
k_e (h^{-1})	1.54	3.3
V_c (mL/kg)	53.2	5.8
k_{on} ($nM^{-1}h^{-1}$)	11.3	15.5
k_{int} (h^{-1})	2.05	14.7
k_{deg} (h^{-1})	0.566	14.3
R_m (nmol/kg)	0.282	10.8
R_m' (nmol/kg)[a]	0.058	21.9
k_{a1} (h^{-1})	0.279	5.75
$k_{a2(10)}$ (h^{-1})[b]	0.454	16.6
$k_{a2(20)}$ (h^{-1})[b]	3.00	43.8
$k_{a2(50)}$ (h^{-1})[b]	3.96	22.6

[a] R_m value for 750 µg/kg IV dose

[b] k_{a2} values vary for each SC dose level

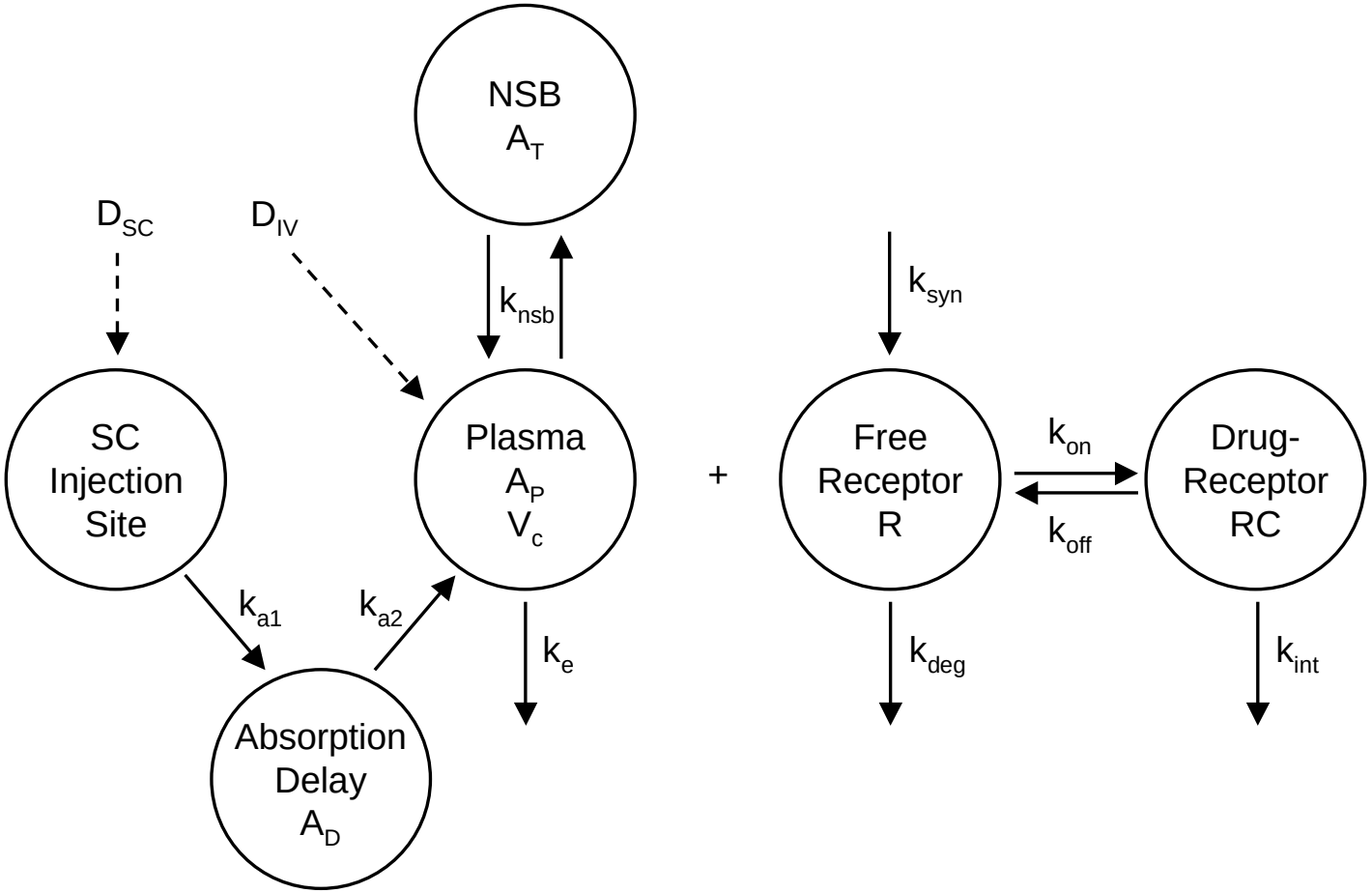

Figure 1

JPET Fast Forward. Published on February 10, 2004 as DOI: 10.1124/jpet.103.063289
This article has not been copyedited and formatted. The final version may differ from this version.

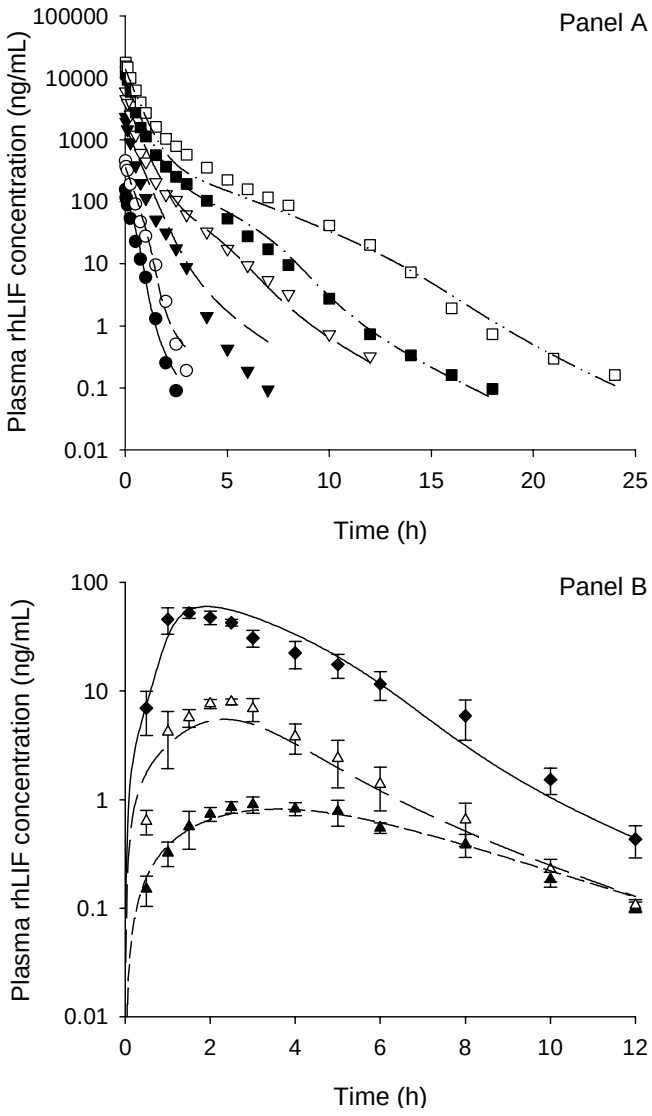

Figure 2

JPET Fast Forward. Published on February 10, 2004 as DOI: 10.1124/jpet.103.063289
This article has not been copyedited and formatted. The final version may differ from this version.

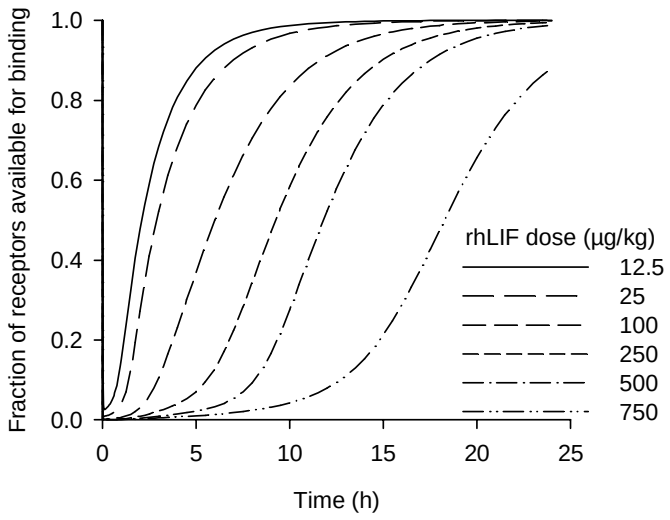

Figure 3